Numerical Simulation on Pulse Ⅱ Ignition Transient Characteristics of Double Pulse Motor

Shan Sun[1,a], Xiong Chen [1,b], Ying-kun Li[1,c] and Liang Zhu[1,d]

[1]School of Mechanical Engineering, NUST, Nanjing 210094, Jiangsu, China

[a]susanedison@163.com,
[b]chenxiong@njust.edu.cn, [c]liyingkun@njust.edu.cn, [d]zhuliang203@123.com

Keywords: Double Pulse Motor; Fluid solid coupling; Solid rocket motor ignition.

Abstract. In this paper, the Ansys Workbench software was used to simulate the fluid structure interaction of the second pulse ignition process in a dual pulse solid rocket motor. The UDF (user define function) was developped through FLUENT software, and the ignition mass flow rate model and the propellant gas adding model during the ignition process were added to the physical model. This paper mainly analyzes the igniter ignition process, propellant surface heat and mass, and igniter propellant gas produced in the layer, interlayer swell and destruction process. The results indicate that the time for interlayer to reach the tensile limit is 1.92ms, and the interlayer failure pressure is 1.44Mpa. The research of this paper provides a reference for the design of the double pulse motor.

Introduction

The dual pulse engine uses an interstage isolator to divide solid rocket engines into two relatively independent combustion chambers. Each propellant charge has an independent combustion chamber and ignition system. The dual pulse engine uses a control system to control the ignition of two combustion chambers. The interval time of two pulses is controlled reasonably so that the energy of the propellant is fully used. To better control and trajectory, significantly improve the offensive system and defense system of weapon system.

In 2004, Schilling S, Trouillot P, Weigand A et al.[1-2] tested the dual pulse engine of 120mm caliber. During the operation of a double pulse engine, the metal diaphragm is normally tearing and the resulting debris is ablated by the high temperature gas. The test proves that the designed dual pulse engine is safe and reliable.

In 2006, Stadler L, Trouillot P, Rien cker C et al.[3] designed by double pulse engine prototype for short-range air defense missile LFK-NG, and ground tests and flight tests are carried out.

In the same year, Naumanne and Stadler et al.[4-6] made and designed a prototype of the dual pulse solid rocket motor for the anti-aircraft missile LFK-NG. In the study, the working state of the metal diaphragm[7], the ignition delay system[8], the heat protection layer and other parts were tested.

In 2012, Javed et al.[9] simulated the internal flow field of the dual pulse engine through the CFX fluid simulation software. Assuming that the metal diaphragm is completely damaged at this time, it is found that there is a large recirculation zone generated by the second pulse during the first pulse combustor, and the pressure and temperature inside the engine are analyzed.

In 2013, Kawadu et al.[10] designed and manufactured a partition double pulse engine. A rubber material is used in the interlayer, and a prefabricated defect is installed in a certain position of the interlayer, which ensures that the double pulse engine can work normally when the second pulse is working.

In 2015, Kim et al.[11] designed and manufactured a hybrid double pulse engine and carried out ground static experiments.

Fluid calculation equation and algorithm

The expression of the ideal gas equation of state is as follows:

$$p = \rho RT \tag{1}$$

In this formula, p, ρ, R, T is the pressure, density, gas constant and temperature of the ideal gas.

The continuity equation expression is as follows:

$$\frac{\partial \rho}{\partial t} + \frac{\partial}{\partial x}(\rho u) + \frac{\partial}{\partial r}(\rho v) + \frac{\rho v}{r} = 0 \tag{2}$$

In this formula, ρ, v is the fluid density and the velocity vector.

The expression of the momentum conservation equation is as follows:

$$\frac{\partial(\rho u_i)}{\partial t} + \frac{\partial}{\partial x_k}(\rho u_i u_k) + \frac{\partial p}{\partial x_i} = \frac{\partial(\tau_i)_k}{\partial x_i} + S_{f_i} \tag{3}$$

The expression of the energy equation is as follows:

$$\frac{\partial(\rho E)}{\partial t} + \frac{\partial}{\partial x_k}(\rho u_k H) = -\frac{\partial}{\partial x_k}(u_j \tau_j)_k + \frac{\partial q_k}{\partial x_k} + S_h \tag{4}$$

The expression of the turbulence model is as follows:

$$\frac{\partial(\rho\kappa)}{\partial t} + \frac{\partial(\rho\kappa\mu_i)}{\partial x_i} = \frac{\partial}{\partial x_j}\left[\left(\mu + \frac{\mu_t}{\sigma_\kappa}\right)\frac{\partial \kappa}{\partial x_j}\right] + G_\kappa + G_b - \rho\varepsilon - Y_M + S_\kappa \tag{5}$$

$$\frac{\partial(\rho\varepsilon)}{\partial t} + \frac{\partial(\rho\varepsilon\mu_i)}{\partial \mu_i} = \frac{\partial}{\partial x_j}\left[\left(\mu + \frac{\mu_t}{\sigma_\varepsilon}\right)\frac{\partial \varepsilon}{\partial x_j}\right] + C_{1\varepsilon}\frac{\varepsilon}{\kappa}(G_\kappa + C_{3\varepsilon}G_b) - C_{2\varepsilon}\rho\frac{\varepsilon^2}{\kappa} + S_\varepsilon \tag{6}$$

$$G_\kappa = \mu_t\left(\frac{\partial \mu_i}{\partial x_j} + \frac{\partial \mu_j}{\partial x_i}\right)\frac{\partial \mu_i}{\partial x_j} \tag{7}$$

$$G_b = \beta g_i \frac{\mu_t}{\mathrm{Pr}_t}\frac{\partial T}{\partial x_j} \tag{8}$$

In this formula, G_κ represents the generating term of turbulent kinetic energy due to the average velocity gradient. G_b is a generating term of turbulent kinetic energy caused by buoyancy. $\mathrm{Pr}_t, \beta, Y_M$ is a turbulence Prandt constant, expansion coefficient and dissipation caused by pulsating expansion in a compressible fluid.

Numerical simulation model

This paper mainly deals with the impulse ignition process of a double pulse engine with an insulating layer. Including igniter ignition, gas transmission, second pulse propellant surface heat and mass and the process of deformation and fracture of interlayer under the pressure of flow field. Fig. 1 is the structure picture of double pulse engine in this article.

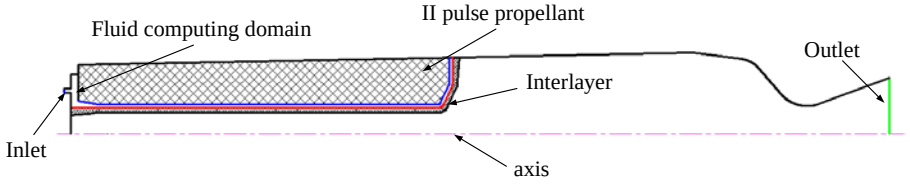

Figure 1. Double pulse engine structure

The deformation and displacement of the propellant charge of the second pulse propellant during the impact process of the second pulse ignition are not considered. The process of propellant charging and charging in the process of impulse ignition shock is studied. Therefore, the charging of the second pulse propellant is simplified as a very thin layer of adding material. Gas adding layer and Fluid between second pulse propellant and interlayer as the research object of the liquid, interlayer as the research object of the solid. Under the condition of ensuring the accuracy of the calculation results, Fig. 2 is shown as a simplified model.

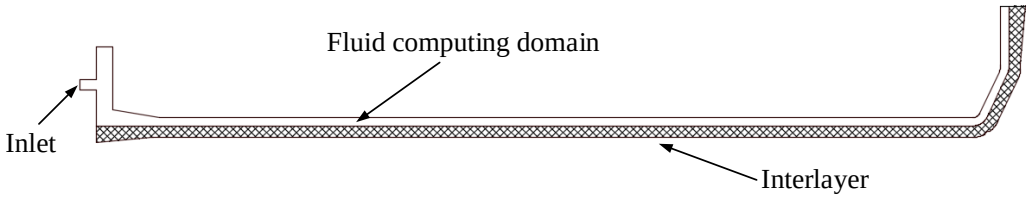

Figure 2. Simplified calculation model

The second pulse column is a single hole tubular drug column, the inner hole and the front and rear end are the burning surface. The maximum length is 532mm, and the inner radius is 42mm. The distance between the interlayer and the second pulse column was 5mm, the radius of the annular igniter is 6mm. The material of interlayer is EPDM, the thickness is 7mm, and the inner radius is 35mm. Interlayer is divided into interlayer cylinder section, interlayer bend cone section, and interlayer end thickening section. There is a Prefabricated defect at the junction of the interlayer cylinder section and the bending cone section. The interlayer is deformed under the pressure of flow field when the second pulse works. When a certain pressure is reached, there is a crack in Prefabricated defect. If Prefabricated defect is not set, the interlayer break time is prolonged, the rupture position is unpredictable, which may impede the normal work of the second pulse engine.

Boundary conditions and initial conditions

Boundary and initial conditions play a very important role in fluid simulation. In this paper, the initial pressure and initial temperature of the simulation model are atmospheric pressure and normal temperature, the pressure is 101325Pa and the temperature is 300K. The total temperature of Igniter gunpowder gas is 2960K, and the initial velocity of gas in all directions is zero. In the calculation area of the flow field, the side wall, the second pulse combustion chamber wall, the propellant charge and the inner wall of the gas adding layer are the adiabatic solid wall boundary conditions. According to the theory of surface layer, the phase gradient of the fixed wall pressure method is equal to zero. According to the gas equation of state, the gradient of the wall density of the fixed wall is equal to zero.

Set the annular Igniter nozzle as the mass flow rate boundary condition. The curve of the engine pressure with time is obtained by the experimental data. The free volume method is used to simulate the mass flow rate of Igniter with time. The UDF (user defined function) is written as the boundary condition of the Igniter entrance through the FLUENT software.

The gas adding layer of a second pulse propellant charge is assumed to be a thin layer on the surface of the propellant. When the gas adding layer grid unit does not reach 750K, the unit does not produce gas, and it is considered as a non slip adiabatic wall. When the gas adding layer grid unit reaches or exceeds 750K, the unit becomes the addition source term and inputs the mass, momentum and energy into the internal flow field.

The two ends before and after setting up interlayer are fixed, and there are no displacements in all directions. The internal flow field and the interlayer contact surface are respectively set as fluid solid coupling data exchange surface, and the data exchange is carried out by using the system couple module in workbench, and the time step is set to 1e-5s. The physical properties of interlayer, propellant and gas are in the Table 1.

Table 1 Parameters of ignition transient simulation in a dual pulse solid rocket motor

Parameter	Value
Specific heat ratio of the propellant gas γ	1.19
Molecular weight of the propellant gas	0.022 [kg/mol]
Burning rate exponent of the propellant n	0.314
Propellant density ρ_p	1800 [kg/m^3]
Burning rate coefficient of the propellant a	1.507×10^{-4}
Thermal conductivity of the propellant λ_s	0.21 [W/(m·K)]
Critical ignition temperature of the propellant	750 [K]
Stagnation temperature of the propellant gas T_0	3200 [K]
Specific heat of the propellant C_s	2256.7 [J/(kg·K)]
Density of the metal diaphragm ρ_m	2700 [kg/m$^{3]}$
Elastic modulus of the Interlayer E_s	25 [MPa]
Poisson ratio of the Interlayer υ	0.49
Stress limit of the Interlayer	8 [MPa]

Results and discussion

From Fig. 3 , we can see that with the increase of igniter gas and the injection of second pulse propellant gas, the pressure inside the channel will suddenly increase, the interlayer will gradually deform and expand, and the gas will fill up the larger area. At last, the prefabricated defect reaches the tensile limit of 8Mpa, and the maximum pressure in the combustion chamber reaches about 1.45Mpa at 1.92ms.

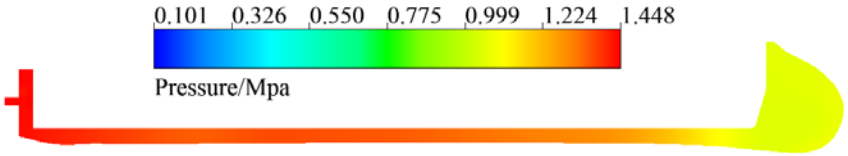

Figure 3. Pressure in the region of the flow field at 1.92ms

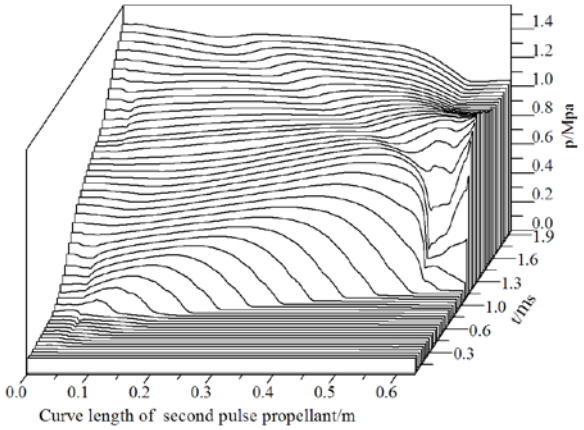

Figure 4. Pressure distribution curve along the length of second pulse propellant at different time

As shown in Fig. 4 , the surface of the second pulse propellant contains three parts: the vertical front surface, the inner surface of the inner hole cylinder, and the terminal surface. It is shown in figure XX that after the ignition of igniter, the high temperature gas propagates backwards along the fluid channel, making the propellant charge surface pressure increasing gradually. Because the region of the channel fluid is narrower, the pressure increases rapidly. With the inflow of igniter gas and second pulse propellant additive gas, when the gas reaches the terminal surface of the second

propellant charge, the pressure reaches a higher value, and the fluid channel propagates forward. Because the deformation and expansion of the interlayer, the fluid region continues to increase, and the pressure growth slows down at this time. At the end of 1.92ms, interlayer reaches the tensile limit. At this time, the maximum pressure of the surface of the second pulse propellant is 1.44Mpa, and the crack is produced on the interlayer.

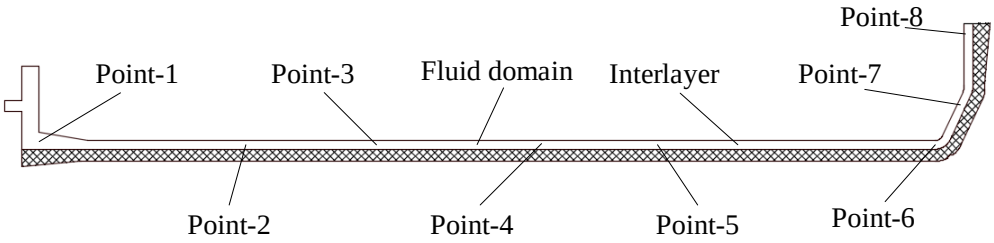

Figure 5. Pressure detection point of fluid domain in second pulse combustion chamber

As shown in Fig. 5 , 8 monitoring points are taken in the flow field of the second pulse combustion chamber. The curves of pressure changes with time at 8 monitoring points are shown in Fig. 6 . It can be seen from the picture that the pressure of the monitoring point in the fluid channel rises in sequence during the ignition process of the second pulse. Interlayer is destroyed at 1.92ms time.

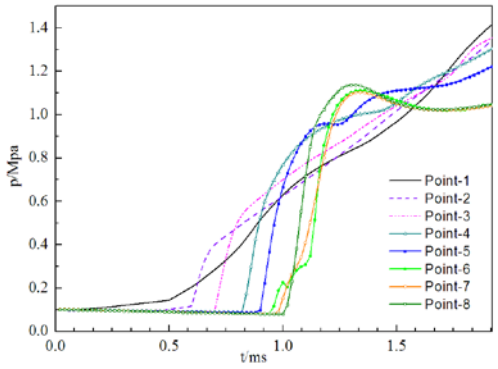

Figure 6. The variation curve of the pressure of the monitoring point with time

Summary

In this paper, the ANSYS Workbench commercial software is used to simulate the transient process of II pulse ignition. The flow field development, the wall pressure variation curve and the interlayer deformation mechanical characteristics during the ignition process are analyzed. The failure time and the failure pressure of interlayer were obtained.

The results of the study show that after the launch of II pulse igniter, at the front of the fluid channel, the high temperature gas becomes a jet. The front end of the propellant is first ignited. The propellant surface starts to burn up and the combustion flame is propagating in the propellant and interlayer channel. The propellant has no burning surface to be ignited and the pressure in the channel increases gradually. Interlayer begins to deform and swell and gas fills the swell area continuously. As time goes on, interlayer is destroyed after the failure criterion is reached.

References

[1] S. Schilling, P. Trouillota and A. Weigand. On the Development and Testing of a 120 mm Caliber Double Pulse Motor (DPM)[M]. 2013.

[2] K. Naumann, L. Stadler and P. Trouillot, et al. Double-Pulse Solid Rocket Technology at Bayern-Chemie/Protac[J]. Aiaa Journal, 2006.

[3] L. Stadler, C. Trouillot Pand Rienäcker, et al. The Dual Pulse Motor for LFK NG[C]// Aiaa/asme/sae/asee Joint Propulsion Conference & Exhibit. 2006.

[4] K. Naumann, L. Stadler and P. Trouillot, et al. Double pulse solid rocket technology at Bayern-Chemie/Protac[R]. AIAA Paper, 2006-4761, 2006.

[5] L. Stadler, S. Hoffmann and H. Niedermaier, et al. Testing and verification of the LFK NG dual pulse motor[R]. AIAA Paper, 2006-4765, 2006.

[6] L. Stadler, P. Trouillot and C. Rienäcker, et al. The dual pulse motor for LFK NG[R]. AIAA Paper, 2006-4762, 2006.

[7] L. Stadler, D. Audri and S. Ruiz, et al. Design of internal insulation and structures for the LFK-NG double pulse motor[R]. AIAA Paper, 2006-4763, 2006.

[8] A. Hacker, R. Stingl and H. Niedermaier, et al. The safety and delay device for the LFK-NG double-pulse motor demonstrator[R]. AIAA Paper, 2006-4764, 2006

[9] A. Javed, P. Manna and D. Chakraborty. Numerical simulation of a dual pulse solid rocket motor flow field[J]. Defence Science Journal, 2012, 62(6): 369-374.

[10] H. Kawadu, I. Yamaguchi and S. Hajiwara, et al. Pulse rocket motor[P]. United States Patent: 0111874, 2013-05-09.

[11] J. Kim, T. Kwon and W. Lee. The design & analysis of pulse separation device with thermal barrier type for dual pulse rocket motor[J]. Journal of the Korean Society of Propulsion Engineers, 2015, 18(1): 93-99.